Magnetization reorientation in $Ga_xMn_{1-x}As$ films: Planar Hall effect measurements

Sunjae Chung and Sanghoon Lee*
Physics Department, Korea University, Seoul 136-701, Korea

X. Liu and J. K. Furdyna
Physics Department, University of Notre Dame, Notre Dame, Indiana 46556, USA

(Received 26 November 2009; revised manuscript received 11 March 2010; published 19 April 2010)

The process of magnetization reorientation in a ferromagnetic semiconductor GaMnAs films was investigated using planar Hall effect measurements. In addition to the well-known two-step switching behavior that occurs during this process, we have observed two additional distinct features in field scan data of the planar Hall resistance (PHR). First, the region of the external field required to begin and complete the reorientation of magnetization from one easy axis to another strongly depends on the direction of the applied field. And second, the maximum amplitude of PHR is significantly reduced during magnetization reversal when the applied field is oriented near one of the easy axes of the GaMnAs film. We provide an explanation of these phenomena using the magnetic field dependence of the free-energy density and assuming the coexistence of multiple domains with three different directions of magnetization in the sample.

DOI: 10.1103/PhysRevB.81.155209 PACS number(s): 75.50.Pp, 75.70.−i, 75.60.−d, 75.47.−m

I. INTRODUCTION

The ferromagnetic semiconductor GaMnAs has recently been receiving a great deal of attention due to the possibilities which it offers for spintronic applications.[1,2] The properties of this material have already been studied extensively by structural,[3,4] optical,[5–7] magnetic,[8–10] and electrical characterization techniques.[11–14] Among those experimental methods, magnetotransport measurements have served as a powerful tool for studying the process of magnetization reorientation in GaMnAs films due to their high sensitivity to the direction of magnetization within this ferromagnetic system. Here the planar Hall effect (PHE), which depends on the angle between the magnetization and the current direction, has proven to be particularly useful in the study magnetic anisotropy, which governs the process of magnetization reorientation during field reversal in GaMnAs films.[11,15]

The two-step switching behavior observed in PHE in GaMnAs films is now well understood as the sequential reorientation of magnetization in 90° steps in a system with four in-plane easy axes that originate from the strong cubic magnetic anisotropy in this material.[16] In addition, there are other noticeable features appearing in the reversal of magnetization in GaMnAs films. For example, the field region required for the reorientation of magnetization between the adjacent easy axes strongly depends on the direction of the applied field. Moreover, the maximum amplitude of the planar Hall resistance (PHR) is significantly smaller when the data are taken with the field applied near one of the easy axes than for fields applied away from the easy axes. Although these features are commonly observed in PHE measurements on GaMnAs films, they have not been discussed in the literature.[11,15,17–19] In this paper we focus on these two phenomena. Specifically, we show that the above effects observed in PHR during magnetization reorientation can be understood by analyzing the magnetic free energy and magnetic domain structure when the concept of nucleation and propagation of the domains is included in the analysis.

II. SAMPLE FABRICATION AND EXPERIMENTAL PROCEDURE

Ferromagnetic GaMnAs films with Mn concentrations of 3.1% and 6.2% were grown at 250 °C on (001) GaAs substrates in a Riber 32 R&D molecular-beam epitaxy machine to thicknesses of 100 nm. A 6×4 mm^2 rectangular piece was cleaved from each GaMnAs sample. For transport measurements, a Hall bar was then patterned on this piece using photolithography and chemical wet etching. The Hall device was in the shape of a 300×1500 μm^2 rectangle, with the long dimension along the $[1\bar{1}0]$ crystallographic direction, and with six terminals for signal detection. The Curie temperatures T_C for the films with 3.1% and 6.2% Mn were estimated from the temperature dependences of their resistivities to be 50 and 62 K, respectively.[20,21] As expected, the Hall measurements revealed that the easy axes are in the plane of the sample. For investigating the PHE, the sample was mounted in a holder designed such that a magnetic field could be applied in the plane of the sample at an arbitrary azimuthal angle φ_H. In the data presented in this paper φ_H is always measured counterclockwise from the $[1\bar{1}0]$ crystallographic direction.

III. DEPENDENCE OF THE RATE OF MAGNETIZATION TRANSITIONS ON APPLIED FIELD DIRECTION

Figure 1 shows field scans of the PHR observed on the two GaMnAs films at 4 K for different orientations φ_H of the external magnetic field H. In addition to the two-step switching behavior, the PHR data of the two films shows conspicuous differences in the transition rate dR_{PHR}/dH at the first and second transitions (i.e., first and second reorientations of the magnetization direction), as indicated by the shaded regions in Fig. 1. In the PHR data taken with $\varphi_H=20°$ (see second row of left column in the figure), the first transition is completed within a very narrow field region while the second transition takes place over a much broader field range. The

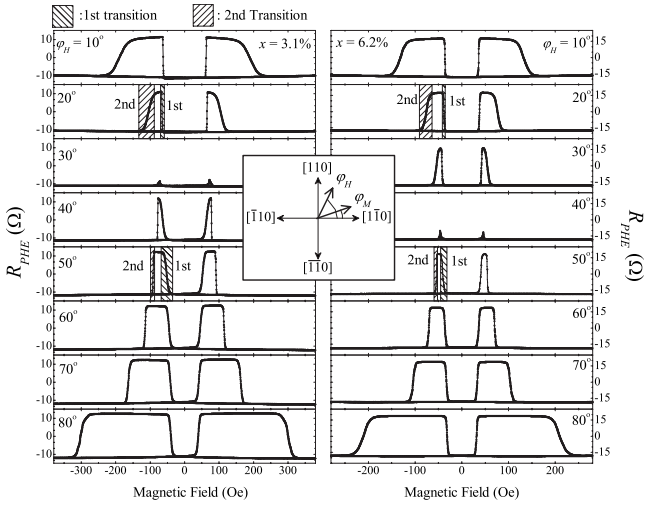

FIG. 1. Field scans of the PHR measured at 4 K for two GaMnAs films at several field directions φ_H. The PHR data shown in left and right columns were obtained for the 3.1% and 6.2% samples, respectively. A clear difference in the transition rate for the first and the second reorientations of magnetization is seen in the PHR data of both samples. The conspicuous reduction in the PHR amplitude is also observed for fields near the easy axis of the film. The crystallographic directions and the angles for the external field and the magnetization used in the measurements shown in the inset.

situation for the two transitions is reversed for the field direction with $\varphi_H=50°$ (i.e., the first transition now occurs over a wider field region than the second transition), as seen, e.g., in the fifth row of Fig. 1.

This behavior of the PHR transitions can be understood in terms of the magnetic free-energy density E_{free} given by[16,22]

$$E_{free}/M = \frac{H_u}{2}\sin^2\varphi + \frac{H_c}{8}\cos^2 2\varphi - H\cos(\varphi-\varphi_H), \quad (1)$$

where H is the external magnetic field; M is the magnetization; H_u and H_c are the uniaxial and cubic anisotropy fields, respectively; and φ and φ_H are angles of magnetization and of the applied magnetic field measured from the $[1\bar{1}0]$ crystallographic direction (i.e., from the direction of the current). The values and angular positions of local minima of the magnetic free-energy density E_{free} given by Eq. (1) determine the direction of magnetization in the system for any given applied field orientation. To locate these minima one must know the values of H_u and H_c for the system of interest.

It is now well established that the magnetic anisotropy fields for a GaMnAs film can be obtained by fitting the angular dependence of the PHR data.[23–25] By following the measurement and analysis procedure demonstrated in Refs. 24 and 26, we obtained the values of $H_u=393$ Oe (150 Oe) and $H_c=1182$ Oe (850 Oe) for the uniaxial and cubic anisotropy fields, respectively, for the 3.1% (6.2%) samples. These anisotropy fields allow us to calculate the free-energy density profile for our GaMnAs layer for different strengths and directions of the applied field H. In Fig. 2 we plot the calculated progression of the energy density profiles with increasing magnetic field for two representative field orientations, $\varphi_H=20°$ and $\varphi_H=50°$, for the 3.1% sample. Although the presence of H_u leads to a slight deviation (about 9.7°) of the magnetic easy axes from the in-plane ⟨100⟩ directions,[16,23] in discussing the behavior of PHR investigated in this study we will for convenience refer to the easy axes of the film simply as the ⟨100⟩ directions.

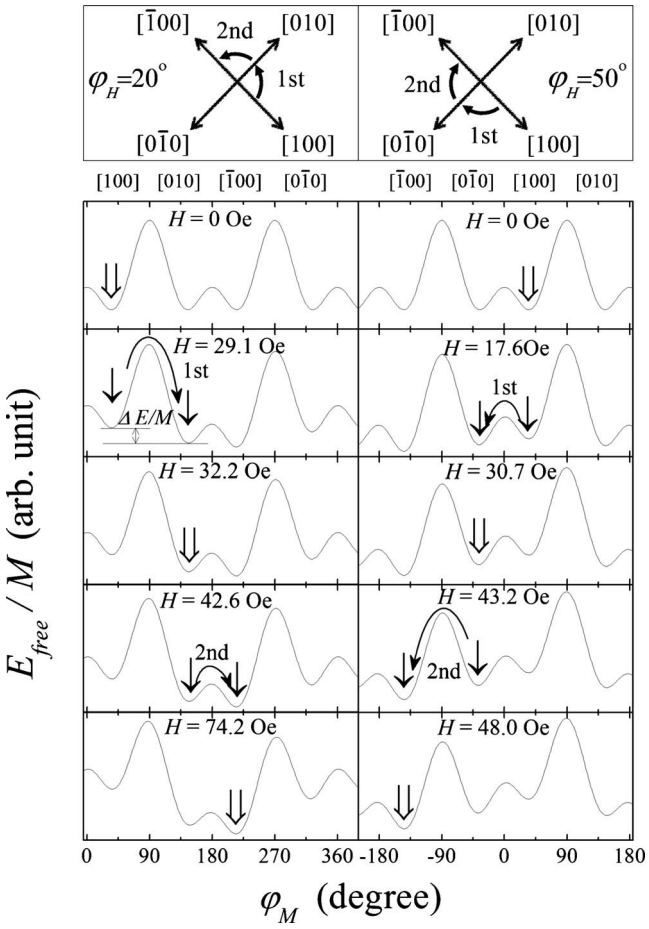

FIG. 2. Evolution of magnetic free-energy density with increasing field in reverse direction for $\varphi_H=20°$ (left column) and $\varphi_H=50°$(right column) for the 3.1% sample. The corresponding first and second transitions are schematically shown at the top of each column. The arrows on the minima indicate the directions of magnetization in the sample at the given field.

The reorientation of magnetization depends on the relative depths of the minima in the magnetic free-energy density given by Eq. (1) and illustrated in Fig. 2 for the 3.1% sample.[26] The energy density differences between neighboring minima, $\Delta E_{free}/M=(E_{free}^{Min1}-E_{free}^{Min2})/M$, can be found for different field strengths and orientations from plots such as those shown in Fig. 2. As an illustration, in Fig. 3 we show calculated values of $\Delta E_{free}/M$ obtained for the field directions $\varphi_H=20°$ and 50° for the GaMnAs sample with 3.1% (upper panels) and 6.2% Mn concentration (lower panels). In the left-hand column of Fig. 3, the solid and open symbols represent the values of $\Delta E_{free}^{[110]}/M=(E_{free}^{[100]}-E_{free}^{[010]})/M$ and $\Delta E_{free}^{[\bar{1}10]}/M=(E_{free}^{[010]}-E_{free}^{[\bar{1}00]})/M$ for the first and second reorientations of magnetization $\boldsymbol{M}$ obtained for $\varphi_H=20°$ (as shown schematically on top left of Fig. 2). One can see that

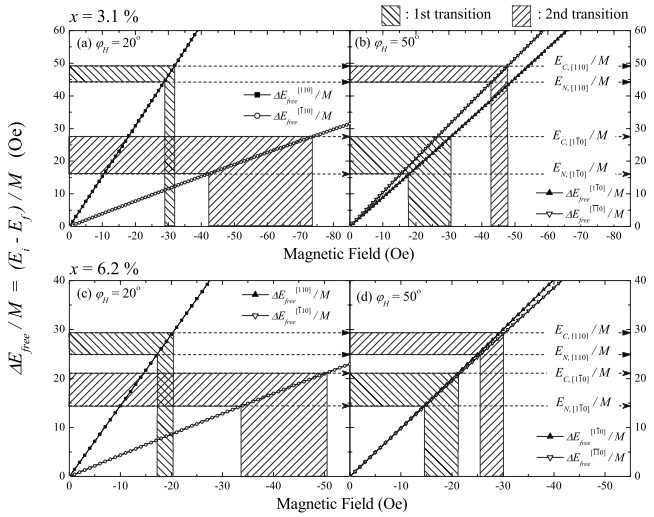

FIG. 3. Difference of free-energy density $\Delta E_{free}/M$ between two neighboring energy minima involved in the reorientation as a function of magnetic field for two field directions, φ_H=20° (right column) and φ_H=50° (left column) for the 3.1% and 6.2% samples. The solid and open symbols represent $\Delta E_{free}/M$ related to the first and the second reorientations, respectively. It is clear that the slopes of $\Delta E_{free}/M$ for the two reorientations are different, although both of them show a linear dependence on the field. The $E_N/M-E_C/M$ for crossing the $[1\bar{1}0]$ and [110] axes are shown as shaded regions.

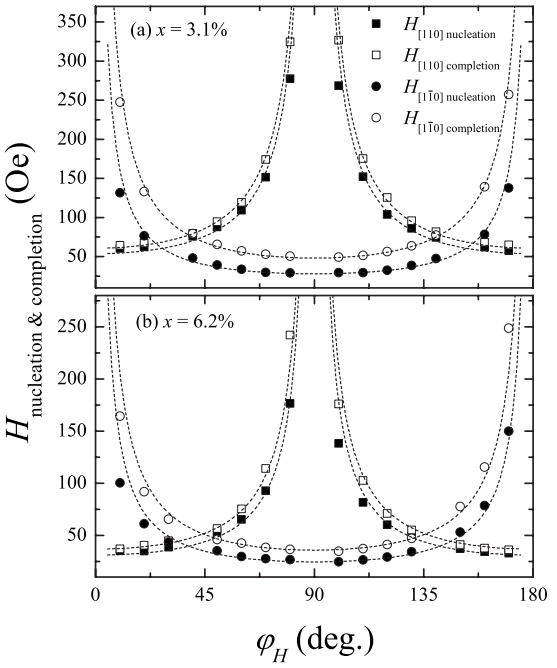

FIG. 4. Angular dependence of H_N and H_C obtained from field scans of PHR for the 3.1% and 6.2% samples shown in Fig. 1. The circles and squares are used for reorientations of magnetization as it crosses the $[1\bar{1}0]$ and [110] axes, respectively. The solid and the open symbols represent H_N and H_C for each reorientation. Dashed lines are fitting curves from which the values of E_N/M and E_C/M were obtained using the methods demonstrated in Refs. 26 and 28.

for this φ_H the value of $\Delta E_{free}/M$ for the first reorientation (i.e., when $\boldsymbol{M}$ crosses the [110] axis, shown by solid symbols) increases faster with magnetic field than for the second (i.e., when $\boldsymbol{M}$ crosses the $[\bar{1}10]$ axis shown by open symbols). In the right-hand column of Fig. 3 the solid and open symbols represent the values for $\Delta E_{free}^{[1\bar{1}0]}/M=(E_{free}^{[100]}-E_{free}^{[0\bar{1}0]})/M$ and $\Delta E_{free}^{[\bar{1}10]}/M=(E_{free}^{[0\bar{1}0]}-E_{free}^{[\bar{1}00]})/M$, respectively, for the first and the second reorientations of magnetization $\boldsymbol{M}$ when the field is applied at φ_H=50° (shown schematically on top right of Fig. 2). For this field direction the behavior is different from that for φ_H=20°: now the first reorientation (corresponding to crossing of the $[1\bar{1}0]$ axis) proceeds at nearly the same rate as the second (when $\boldsymbol{M}$ crosses the $[\bar{1}\bar{1}0]$) for both samples. From the magnetic field dependence of $\Delta E_{free}/M$ for the two reorientations illustrated in Fig. 3 for φ_H=20° or 50° one can qualitatively understand the reason for the opposite behavior of the first and the second transition rates seen in the field scans of PHR in Fig. 1 for these field orientations.

For a more complete description of such PHR transitions, however, one must also know the domain nucleation field E_N/M and the completion field E_C/M of the transition, i.e., fields that correspond to the start and the end of the reorientation, respectively. The angular dependences of the start and the end fields of the two transitions can be obtained from the data shown in Fig. 1 and we plot them as open and solid symbols in Fig. 4. In analogy with the method of finding domain pinning fields demonstrated in Refs. 24 and 26–28, the angular dependences of the start and the end fields of a given reorientation can be fitted using the free-energy model to obtain E_N/M and E_C/M, as shown in Fig. 4. From these fits we obtained the values of E_N/M and E_C/M for the two samples for crossing the $[\bar{1}10]$ and [110] axes. For the 3.1% sample, E_N/M and E_C/M were found to be 16.09 and 27.53 Oe for crossing the $[\bar{1}10]$ axis, and 44.26 and 49.14 Oe for crossing the [110] axis. In the case of 6.2% sample, E_N/M and E_C/M were found to be 14.41 and 21.11 Oe for crossing the $[\bar{1}10]$ axis, and 24.9 and 29.37 Oe for crossing the [110] axis.

When the direction of magnetization crosses the [110] and $[\bar{1}10]$ axes, this corresponds to the first and the second reorientations in the panels in row 2 of Fig. 1. The reorientation sequence is reversed in the fifth row of Fig. 1, i.e., crossing the [110] axis now corresponds to the second reorientation, and crossing of $[\bar{1}10]$ to the first (see top panels of Fig. 2). In Fig. 3 we have shaded the regions of $(E_N-E_C)/M$ representing the full reorientation process across the [110] and $[\bar{1}10]$ directions. As soon as the $\Delta E_{free}/M$ for a given magnetic field direction becomes larger than the domain nucleation field E_N/M, a new magnetic domain will begin to nucleate and expand until it occupies the entire area of the sample at the value of E_C/M.[29,30]

In the left-hand column of Fig. 3, it is clear that with field oriented at φ_H=20° a wider field range is required to start and complete the second reorientation of magnetization, $[010]\rightarrow[\bar{1}00]$ (i.e., crossing the $[\bar{1}10]$ axis), than the first reorientation, $[100]\rightarrow[010]$ (i.e., crossing [110]), as seen in the second row of Fig. 1. The situation is different when the

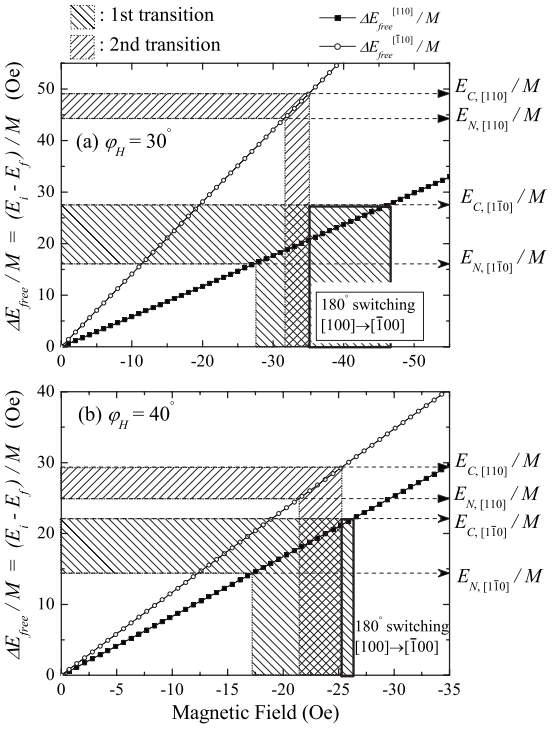

FIG. 5. Magnetic field dependence of $\Delta E_{free}/M$ for the condition when R_{PHE} nearly vanishes in Fig. 1 (φ_H=30° for the 3.1% sample and 40°, 6.2%). Unlike the cases for φ_H=20° and 50° shown in Fig. 3, the first and the second reorientations in both the upper (3.1% sample) and lower panel (6.2% sample) *overlap* in a certain field region, indicating a coexistence of multiple domains with three different directions. In the field region between 35 and 47 Oe for the 3.1% sample, and between 25 and 28 Oe for 6.2% sample, the reorientation occurs directly from the [100] to the [$\bar{1}$00] direction by a 180° rotation.

field direction is φ_H=50°, as seen in the right-hand column of Fig. 3, where a wider field region is needed for completing the first reorientation (i.e., for crossing [1$\bar{1}$0]) than for the second reorientation (i.e., for crossing the [$\bar{1}\bar{1}$0] axis). This leads to a broader field region for the first transition than for the second in the PHR measured for φ_H=50°, as seen in the fifth row of Fig. 1.

IV. COEXISTENCE OF THREE DIFFERENT DIRECTIONS OF MAGNETIZATION

Another noticeable feature of the PHR data shown in Fig. 1 is the striking line shape change and reduction in the magnitude of PHR during reorientation as φ_H approaches one of the easy axes of GaMnAs (see, e.g., data taken at φ_H=30° and 40° for the 3.1% and 6.2% samples, respectively, in Fig. 1). The concept of nucleation and propagation of magnetic domains also provides an understanding of this behavior. The magnetic field dependence of the energy density differences between two neighboring minima of the free energy (i.e., $\Delta E_{free}/M$) for the two samples are shown in Fig. 5 for φ_H =30° (for the 3.1% sample) and 40° (6.2% sample). The solid and open symbols represent $\Delta E_{free}/M$ for the first and the second reorientations, respectively, and the regions of $E_N/M - E_C/M$ for the two reorientations are indicated as shaded areas in the figure. Unlike cases for φ_H=20° and for φ_H=50° in Fig. 3, in which the first and the second magnetization reorientations take place from start to finish in two well-separated magnetic field regions in Fig. 5 we see that the field regions for the two reorientations overlap. This indicates that the second reorientation (i.e., from [010] to the [$\bar{1}$00]) begins *before* the first reorientation (i.e., from the [100] to the [010]) is completed in the entire area of the sample. Thus during the magnetization reversal for this φ_H three directions of magnetization (along [100], [010], and [$\bar{1}$00]) will coexist within the sample as the field is being reversed. This is represented by the overlapping crosshatched area in Fig. 5. Such reorientation phenomena involving three coexisting directions of magnetization have already been observed by magneto-optical imaging in earlier studies.[5]

The coexistence of domains with three different directions of magnetization will be reflected in PHR, because its value is a sensitive function of the direction of magnetization, given by[16,23,31,32]

$$R_{\mathrm{PHE}} = \frac{k}{t} M^2 \sin 2\varphi, \tag{2}$$

where t is the film thickness; φ is the angle between the direction of the current flow and the magnetization M; and k is a constant related to the anisotropic magnetoresistance (i.e., the difference of resistivity for the magnetization parallel and perpendicular to the current direction). Equation (2) indicates that PHR has a maximum (positive) value for magnetizations along the [100] or the [$\bar{1}$00] directions (i.e., φ =45° and φ=225°) while a minimum (negative) value occurs for magnetizations along [010] or [0$\bar{1}$0] (i.e., φ=135° and φ=315°). Therefore, if the first 90° reorientation (i.e., [100]→[010]) is completed in the entire area of the sample before the second 90° reorientation (i.e., [010]→[$\bar{1}$00]) begins, both the maximum and the minimum values of the PHR are fully observed during magnetization reversal, as is seen for field directions far from the magnetic easy axes (e.g., for $\varphi_H \leq 20^\circ$ and for $\varphi_H \geq 50^\circ$ in Fig. 1).

In contrast, in the case when the external field is applied near the magnetic easy axes (e.g., along the [100] direction), the Zeeman energy due to the field has the strongest effect on the free energy for the opposite direction (i.e., [$\bar{1}$00]). This makes the energy minimum corresponding to the reversed direction (i.e., to [$\bar{1}$00]) much deeper than that corresponding to the intermediate [010] direction (i.e., that of the magnetic easy axis orthogonal to [100]). Therefore, as the first transition of 90° (i.e., [100]→[010]) begins to occur during the process of field reversal, the condition for the second 90° transition (i.e., [010]→[$\bar{1}$00]) is already established due to the deep free-energy minimum for [$\bar{1}$00]. Such free-energy profile results in the two 90° consecutive transitions (i.e., [100]→[010] and [010]→[$\bar{1}$00]) occurring almost on top of each other when the field reversal takes place near an easy axis.

If the second reorientation starts before the first reorientation is completed in the entire sample, during reorientation the sample will consist of areas with magnetization along [100], [010], and $[\bar{1}00]$ directions. The PHR value for such overlapping transition region is then given by the sum of the contributions from all three different directions of magnetic domains, weighted by areas occupied by each of these magnetization orientations. This can be expressed as[32]

$$R_{\mathrm{PHE},normalized} = \frac{R_{\mathrm{PHE}}}{R_{Max}} = (1-p)^2 \sin 2\varphi_1 + (p-p')^2 \sin 2\varphi_2 + p'^2 \sin 2\varphi_3, \quad (3)$$

where R_{Max} is the maximum value of PHR when the magnetization is along either the [100] or the $[\bar{1}00]$ direction in the entire area of the sample and φ_n are the directions of the easy axes given as $\pi/4+(n-1)\pi/2$. If we consider magnetization reorientation from [100] to $[\bar{1}00]$, as is the case for $\varphi_H = 30°$ for the 3.1% sample, then φ_1, φ_2, and φ_3 correspond to magnetizations along the [100], [010], and $[\bar{1}00]$ directions, respectively. In Eq. (3) p and p' are portions of the sample area occupied by domains magnetized along the [010] and the $[\bar{1}00]$ directions, respectively, and can vary between 0 and 1. One can see from Eq. (3) that for the case of magnetic multidomains with nonzero p' the PHR cannot attain its maximum value during reorientation from the [100] to the $[\bar{1}00]$ direction. Such reduction in PHR caused by multidomains with three different directions of magnetizations that occur simultaneously when the field is applied close to one of the easy axes, as can be seen very nicely in the PHR data observed at $\varphi_H = 30°$ and 40° for two samples, respectively, in Fig. 1.

It is also interesting to note in Fig. 5 that the second reorientation (i.e., [010]→$[\bar{1}00]$) can be completed even before the completion of the first reorientation (i.e., [100]→[010]). Once the second reorientation is completed, the area with magnetization along the [010] direction disappears and only two magnetic domains (along the original [100] and the final $[\bar{1}00]$ directions) are involved in the rest of the reversal process. Therefore, after completion of the second reorientation, the reversal of magnetization occurs directly by a 180° rotation from the [100] to the $[\bar{1}00]$ direction This corresponds to the field region between 35 and 47 Oe in the upper panel and to the field region between 25 and 28 Oe in the lower panel of Fig. 5.

V. CONCLUSION

We carried out a detailed study of the phenomena occurring in the process of magnetization reorientation in GaMnAs films with dominant cubic anisotropy. Magnetic field scans of PHR showed that the *transition rate* between the maximum and the minimum values of PHR (dR_{PHR}/dH) for the first and the second transition strongly depends on the applied field direction. This phenomenon can be understood by analyzing the magnetic free energy in the presence of the magnetic field, which shows that the energy differences $\Delta E_{free}/M$ between two adjacent energy minima involved in the reorientation of magnetization strongly depend on the direction of the external field. This approach also shows that the observed reduction in the PHR magnitude occurring when the field is applied near one of easy axes arises from the coexistence of magnetic domains with three different magnetization directions. We have also shown that the features observed in the magnetization reorientation process—and particularly the shape of the PHR "steps"—can be qualitatively understood in terms of the nucleation and propagation of domains. It is known, however, that the magnetic domains in a GaMnAs film are also characterized by a distribution of pinning fields.[33] This effect needs to be considered for further quantitative description of magnetization reorientation in the GaMnAs films and of its effect on PHR.

ACKNOWLEDGMENTS

This research was supported by Basic Science Research Program through the National Research Foundation of Korea (NRF) funded by the Ministry of Education, Science and Technology (Grant No. 2009-0057687); by the Seoul R&DB Program (Grant No. 10543); and by the National Science Foundation under Grant No. DMR06-03762.

*slee3@korea.ac.kr

[1] S. A. Wolf, D. D. Awschalom, R. A. Buhrman, J. M. Daughton, S. von Molnar, M. L. Roukes, A. Y. Chtchelkanova, and D. M. Treger, Science **294**, 1488 (2001).
[2] S. Lee, J. H. Chung, X. Y. Liu, J. K. Furdyna, and B. J. Kirby, Mater. Today **12**, 14 (2009).
[3] G. M. Schott, W. Faschinger, and L. W. Molenkamp, Appl. Phys. Lett. **79**, 1807 (2001).
[4] J. H. Chung, S. J. Chung, S. Lee, B. J. Kirby, J. A. Borchers, Y. J. Cho, X. Liu, and J. K. Furdyna, Phys. Rev. Lett. **101**, 237202 (2008).
[5] U. Welp, V. K. Vlasko-Vlasov, X. Liu, J. K. Furdyna, and T. Wojtowicz, Phys. Rev. Lett. **90**, 167206 (2003).
[6] R. Lang, A. Winter, H. Pascher, H. Krenn, X. Liu, and J. K. Furdyna, Phys. Rev. B **72**, 024430 (2005).
[7] L. V. Titova, M. Kutrowski, X. Liu, R. Chakarvorty, W. L. Lim, T. Wojtowicz, J. K. Furdyna, and M. Dobrowolska, Phys. Rev. B **72**, 165205 (2005).
[8] H. Ohno, A. Shen, F. Matsukura, A. Oiwa, A. Endo, S. Katsumoto, and Y. Iye, Appl. Phys. Lett. **69**, 363 (1996).
[9] M. Sawicki, F. Matsukura, A. Idziaszek, T. Dietl, G. M. Schott, C. Ruester, C. Gould, G. Karczewski, G. Schmidt, and L. W. Molenkamp, Phys. Rev. B **70**, 245325 (2004).
[10] M. Sawicki, K.-Y. Wang, K. W. Edmonds, R. P. Campion, C. R. Staddon, N. R. S. Farley, C. T. Foxon, E. Papis, E. Kamińska, A. Piotrowska, T. Dietl, and B. L. Gallagher, Phys. Rev. B **71**,

121302(R) (2005).
[11] F. Matsukura, H. Ohno, A. Shen, and Y. Sugawara, Phys. Rev. B **57**, R2037 (1998).
[12] K. W. Edmonds, K. Y. Wang, R. P. Campion, A. C. Neumann, C. T. Foxon, B. L. Gallagher, and P. C. Main, Appl. Phys. Lett. **81**, 3010 (2002).
[13] S. U. Yuldashev, H. C. Jeon, H. S. Im, T. W. Kang, S. H. Lee, and J. K. Furdyna, Phys. Rev. B **70**, 193203 (2004).
[14] A. Van Esch, L. Van Bockstal, J. De Boeck, G. Verbanck, A. S. van Steenbergen, P. J. Wellmann, B. Grietens, R. Bogaerts, F. Herlach, and G. Borghs, Phys. Rev. B **56**, 13103 (1997).
[15] D. Y. Shin, S. J. Chung, S. Lee, X. Liu, and J. K. Furdyna, Phys. Rev. B **76**, 035327 (2007).
[16] H. X. Tang, R. K. Kawakami, D. D. Awschalom, and M. L. Roukes, Phys. Rev. Lett. **90**, 107201 (2003).
[17] K. Y. Wang, K. W. Edmonds, R. P. Campion, L. X. Zhao, C. T. Foxon, and B. L. Gallagher, Phys. Rev. B **72**, 085201 (2005).
[18] A. M. Nazmul, H. T. Lin, S. N. Tran, S. Ohya, and M. Tanaka, Phys. Rev. B **77**, 155203 (2008).
[19] Z. Ge, W. L. Lim, S. Shen, Y. Y. Zhou, X. Liu, J. K. Furdyna, and M. Dobrowolska, Phys. Rev. B **75**, 014407 (2007).
[20] S. U. Yuldashev, H. Im, V. S. Yalishev, C. S. Park, T. W. Kang, S. Lee, Y. Sasaki, X. Liu, and J. K. Furdyna, Appl. Phys. Lett. **82**, 1206 (2003).
[21] V. Novak, K. Olejník, J. Wunderlich, M. Cukr, K. Výborný, A. W. Rushforth, K. W. Edmonds, R. P. Campion, B. L. Gallagher, J. Sinova, and T. Jungwirth, Phys. Rev. Lett. **101**, 077201 (2008).
[22] E. C. Stoner and E. P. Wohlfarth, Philos. Trans. R. Soc. London, Ser. A **240**, 599 (1948).
[23] D. Y. Shin, S. J. Chung, S. Lee, X. Liu, and J. K. Furdyna, Phys. Rev. Lett. **98**, 047201 (2007).
[24] D. Y. Shin, S. J. Chung, S. Lee, X. Liu, and J. K. Furdyna, IEEE Trans. Magn. **43**, 3025 (2007).
[25] H. Son, S.-J. Chung, S.-Y. Yea, S. Lee, X. Liu, and J. K. Furdyna, J. Appl. Phys. **103**, 07F313 (2008).
[26] R. P. Cowburn, S. J. Gray, J. Ferre, J. A. C. Bland, and J. Miltat, J. Appl. Phys. **78**, 7210 (1995).
[27] S.-Y. Yea, S.-J. Chung, H. Son, S. Lee, X. Liu, and J. K. Furdyna, J. Appl. Phys. **103**, 07D118 (2008).
[28] K. Hamaya, T. Taniyama, Y. Kitamoto, R. Moriya, and H. Munekata, J. Appl. Phys. **94**, 7657 (2003).
[29] A. Dourlat, C. Gourdon, V. Jeudy, C. Testelin, K. Khazen, J. L. Cantin, H. J. von Bardeleben, L. Thevenard, and A. Lemaitre, IEEE Trans. Magn. **43**, 3022 (2007).
[30] K. Y. Wang, A. W. Rushforth, V. A. Grant, R. P. Campion, K. W. Edmonds, C. R. Staddon, C. T. Foxon, B. L. Gallagher, J. Wunderlich, and D. A. Williams, J. Appl. Phys. **101**, 106101 (2007).
[31] S. Lee, D. Y. Shin, S. J. Chung, X. Liu, and J. K. Furdyna, Appl. Phys. Lett. **90**, 152113 (2007).
[32] S. J. Chung, D. Y. Shin, H. Son, S. Lee, X. Liu, and J. K. Furdyna, Solid State Commun. **143**, 232 (2007).
[33] J. Kim, D. Y. Shin, S. Lee, X. Liu, and J. K. Furdyna, Phys. Rev. B **78**, 075309 (2008).